IRAQI JOURNAL OF APPLIED PHYSICS
Vol. 22, No. 3, July-September 2026, pp. 479-484

Structural and Optical Characteristics of Zinc Oxide Nanostructures Deposited by Reactive Magnetron Sputtering: Role of Gas Mixing Ratio

Mohanad A. Aswad*
Firas J. Kadhim

Department of Physics,
College of Science,
University of Baghdad,
Baghdad, IRAQ
* Corresponding author email:
mohannad.abd2404p@sc.uobaghdad.edu.iq

The reactive magnetron sputtering was employed to synthesize zinc oxide (ZnO) nanostructures at different Ar:O_2 gas mixing ratios. The formation of wurtzite phase of ZnO was confirmed with larger crystallinity at higher O_2 ratios and reduced average crystallite size at the highest Ar ratio. The Zn-O stretching vibration besides O-H bending and stretching modes were revealed, indicating higher hydroxyl adsorption at larger oxygen content. The gas ratio was found strongly influencing topographic morphology of ZnO films where the O_2-rich conditions produced finer and more homogeneous nanostructures, whereas Ar-rich deposition promoted grain formation and surface roughness. The prepared material showed stoichiometric composition with no traces for other elements or impurities as well as showed strong UV absorption (350-360 nm) and high transmittance in the visible range. The values of energy band gap (3.56-3.78 eV) were found to decrease with decreasing O_2 ratio, highlighting the importance of reactive magnetron sputtering of the synthesis highly efficient ZnO nanostructures to satisfy the requirements of many applications including photocatalytic and biomedical applications.

Keywords: Zinc oxide; Nanostructures; Reactive sputtering; Gas mixing ratio
Received: 12 October 2025; Revised: 13 January 2026; Accepted: 20 January 2026; Published: 1 July 2026

Introduction

Zinc oxide is a versatile semiconductor metal oxide that has attracted research interest because of its unique combination of electronic, optical, and chemical properties [1]. At ambient conditions ZnO adopts the hexagonal wurtzite structure, in which zinc Zn^{2+} and oxygen O^{2-} ions are arranged in tetrahedral coordination [2]. The simplicity of tunning morphology (from nanoparticles and nanorods to nanosheets and thin films) combined with wide band gap (~3.6eV) makes ZnO an attractive platform across catalysis, photonics, sensor, and biomedical disciplines [3],[4].

A broad field of synthesis techniques has been developed to produce ZnO nanostructures with controlled size, shape, and defect content [5]. Physical and thin films approaches (e.g., sputtering [6], thermal evaporation [7], and pulsed-laser deposition [8]) allow dense, crystalline films for devices fabrication, while chemical methods (e.g., sol-gel [9], hydrothermal [10], and precipitation [11]) are low coast, scalable for colloidal nanoparticles and flexible nanocomposites preparing. Green (bio-assisted) synthesis using plant extracts [12], as reducing agents which have become particularly prominent because they can reduce hazardous reagents and produce ZnO with enhanced biocompatibility [13]. DC reactive magnetron plasma sputtering is an important technology for thin films synthesis because it provides accurate control over the composition and thickness of the films, as well as high deposition rate [14]. In this technology, morphology is primarily governed by sputtering parameters such gas mixing ratio, discharge power, and processing pressure [15]. DC magnetron sputtering versatility enables fabrication of multifunctional nanostructured materials for diverse fields [16]. Nanostructures of ZnO are applicable in numerous applications like electronics [17], photonics [18], and environmental sensing [19]. These key applications include ultraviolet lasers [20], chemical sensors for gas detection [21] and nanogenerators for energy harvesting [22]. They are also widely used in photocatalysis in water purification [23] and antibacterial agents [24].

While ZnO has been frequently synthesized using sputtering, studies that comprehensively investigate how variation in gas mixing ratio influence the structural, morphological, and optical characteristics remain limited. Therefore, the objective of the present work is to synthesize high quality and homogenous ZnO nanostructures via reactive magnetron plasma sputtering and focus on investigation of correlation between sputtering parameters zinc oxide nanostructures characteristics.

Experimental Work

Zinc oxide nanostructures were fabricated via a reactive magnetron plasma sputtering system. A circular zinc sheet target (60 mm in diameter) was used as sputtering cathode, powered by a 3 kV DC power supply. The process was carried out at a process pressure of 7.3×10^{-2} mbar within a vacuum chamber

 © ALL RIGHTS RESERVED

(31 cm diameter, 37 cm height) equipped with a rotary pump. The sputtering environment consisted of a mixture of (99.99%) pure argon and (99.99%) pure oxygen gases. The glass substrates were positioned 40 mm from the target and directly faced it during deposition. Furthermore, it was kept at room temperature. An ultrasonic path was utilized to clean substrates with 99% ethanol at 40°C for 10 min. before the deposition process. They were then rinsed in deionized water for an additional 10 min, and allowed to air dry. The argon-oxygen gas mixtures were introduced at varying ratios: (50:50), (55:45), (60:40), (65:35), (75:25), and (80:20). The deposition was conducted for 1.5 hours at a constant voltage of 700V. A needle valve controlled the steady flow of the gas mixture into the chamber, ensuring consistent pressure throughout the process, which is critical for uniform film formation. Figure (1) shows one of the synthesized ZnO films.

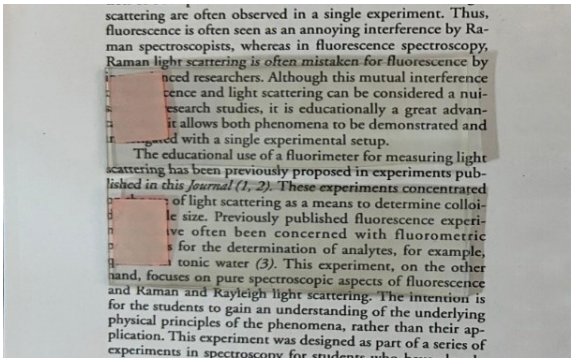
scattering are often observed in a single experiment. Thus, fluorescence is often seen as an annoying interference by Raman spectroscopists, whereas in fluorescence spectroscopy, Raman light scattering is often mistaken for fluorescence by [redacted] researchers. Although this mutual interference [redacted] and light scattering can be considered a nui- [redacted] research studies, it is educationally a great advan- [redacted] it allows both phenomena to be demonstrated and [redacted] with a single experimental setup.

The educational use of a fluorimeter for measuring light scattering has been previously proposed in experiments published in this Journal (1, 2). These experiments concentrated [redacted] of light scattering as a means to determine colloi- [redacted] le size. Previously published fluorescence experi- [redacted] ve often been concerned with fluorometric [redacted] for the determination of analytes, for example, [redacted] tonic water (3). This experiment, on the other hand, focuses on pure spectroscopic aspects of fluorescence and Raman and Rayleigh light scattering. The intention is for the students to gain an understanding of the underlying physical principles of the phenomena, rather than their application. This experiment was designed as part of a series of experiments in spectroscopy for students [redacted]

Fig. (1) Photographs of one of the synthesized ZnO films at a specific gas mixing ratio

The film elemental composition and surface morphology were examined using an Thermo Fisher Scientific Axia ChemiSEM FE-SEM equipped with EDS unit. Crystallographic structure and phase analysis were performed via XRD using a Malvern Panalytical Aries compact diffractometer, while molecular bonding characteristics were analyzed using a Shimadzu FTIR-8400S spectrophotometer. Optical properties were determined using a Shimadzu UV-1800 spectrophotometer at ambient temperature. The spectrum was carried out with a resolution of 1 nm between 200 and 900 nm.

Results and Discussion

The XRD patterns in Fig. (2) of ZnO nanostructures deposited at various Ar:O_2 ratios confirm the formation of hexagonal wurtzite phase (JCPDS card number 36-1451), with all observed diffraction peaks assigned to (100), (002), (101), (102), (110), (103), (200), (112), (201), and (202) planes. The absence of secondary phases indicates that reactive magnetron plasma sputtering enabled the growth of pure phase ZnO under all investigated parameters. A strong dependence of crystallinity on gas mixing ratio is noticed. At Ar-rich parameters, specifically (65:35) and (75:25) exhibit highest intensity suggested enhancement of crystallinity. On the other hand, films synthesized at intermediate (50:50) and (55:45) ratios show a slight reduction in peak intensity, which may be attributed to introduction of oxygen vacancies. Lastly, the (80:20) mixing ratio results in broader peaks indicating smaller crystallite size that is estimated according to Scherrer's equation. Furthermore, the increased value of microstrain for 80:20 ratio arising from oxygen vacancy induced lattice distortion under oxygen deficient sputtering conditions. In addition, the results showed an inverse correlation between the average crystallite size and O_2 content that can be explained by enhancement of Zn adatoms and strong surface diffusion favoring crystallites growth under low oxygen content, while high oxygen content raises nucleation density and restricts surface diffusion yielding smaller ZnO crystallites. These findings proved that optimizing Ar:O_2 ratio is important to tailoring the structural quality of sputtered ZnO films for many desired applications. Three Ar:O_2 mixing ratios was selected with smaller average crystallite size as optimum conditions for further characterization and analysis, which are (50:50), (55:45), and (80:20).

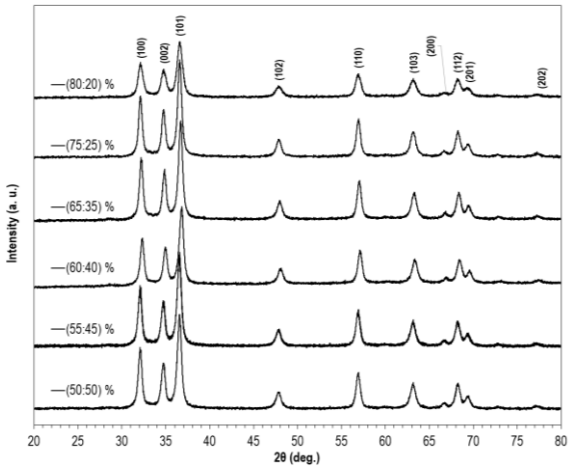

Fig. (2): XRD patterns of prepared zinc oxide films at (50:50), (55:45), (60:40), (65:35), (75:25), and (80:20) Ar:O_2 mixing ratios

Table (1) Estimated average crystalline size and microstrain values for deposited ZnO at different gas mixing ratios

Ar:O_2 %	Average crystallite size (nm)	Macrostrain
50:50	13.4	0.96
55:45	13.2	0.97
60:40	13.9	0.95
65:35	14.0	0.91
75:25	14.5	0.88
80:20	9.7	1.33

FTIR spectra of zinc oxide nanostructures synthesized under selected Ar:O_2 ratios (50:50, 55:45, 80:20) depicted in Fig. (3). All spectra reveal main three features: the fundamental Zn-O stretching

 © ALL RIGHTS RESERVED

vibration (400-600 cm^{-1}), an O-H bending vibration mode (~1620 cm^{-1}), and a broad stretching vibration mode of O-H (3200-3600 cm^{-1}). Confirming formation of ZnO with surface adsorption of hydroxyl groups due to air moisture. Higher oxygen ratio (50:50) promotes hydroxyl rich environment, whereas Ar rich deposition (80:20) yield ZnO nanostructures with minimal hydroxyl contamination. This trend suggests that higher oxygen content creates more oxygen rich surface terminations and dangling bonds which promote adsorption of water molecules from air.

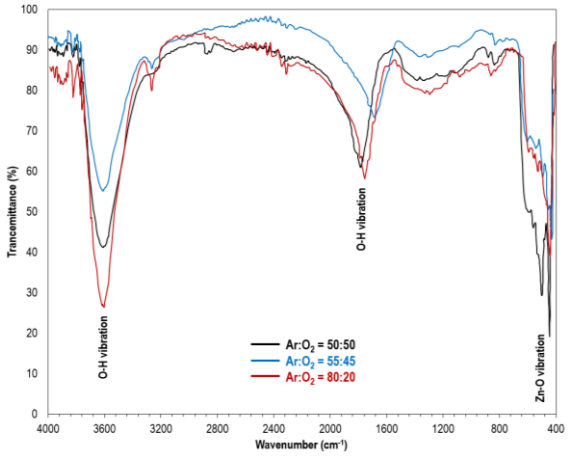

Fig. (3) FTIR spectra of zinc oxide thin film prepared using 50:50, 55:45, and 80:20 mixing ratios of Ar:O_2

FE-SEM images in Fig. (4) show that the morphology of ZnO nanostructures is strongly influenced by Ar:O_2 gas mixing ratio. For (50:50) sample, it can be seen a percentage of agglomerated clusters composed of irregularly shaped particles in the range of 60-90 nm, with a notable pore. Decreasing the oxygen content (55:45) leads to smaller, nearly spherical particles (35-55 nm) with more uniform arrangement and smoother surface. This can be explained by surplus of oxygen can act as scattering centers restricting lateral mobility and favor formation of smaller grains. In contrast, in Ar-rich environment (mixing ratio of 80:20), the higher number of sputtered Zn atoms reaches the substrate leads to higher surface roughness with particles size approaches 40-60 nm because the heavier Ar^+ ions deliver stronger momentum to the film. The transfer of this momentum increases adatom mobility across the substrate allowing atoms to migrate, combine, and form larger grains through coalescence. As a result, the higher oxygen conditions favor finer and more homogeneous nanostructures while argon rich conditions adopt particles growth and surface roughness.

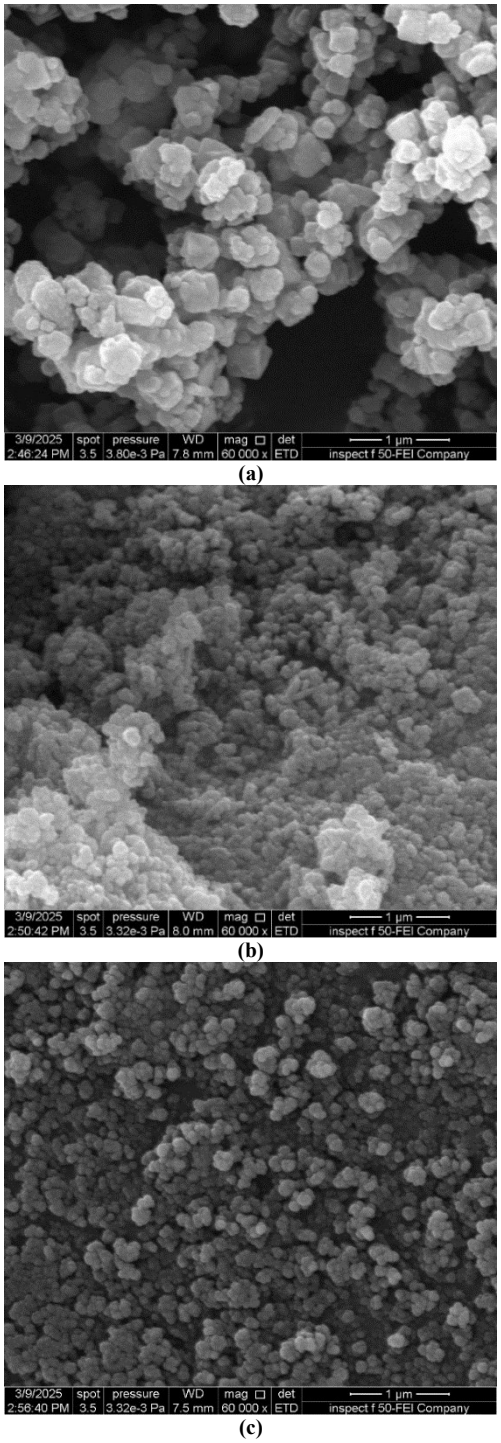

(a)

(b)

(c)

Fig. (4) FE-SEM micrographs of the zinc oxide nanostructures synthesized via DC magnetron plasma sputtering at different gas mixing ratios (a) (50:50) (b) (55:45), (c) (80:20)

EDS spectra showed in Fig. (5) confirmed that all ZnO samples are mainly composed of Zn and O without a noticed impurity, verifying a successful pure zinc oxide nanostructures formation. In addition, EDS supports that all deposited films contain the expected Zn and O elements in near stoichiometric composition consisted with targeted ZnO phase.

 © ALL RIGHTS RESERVED

Table (2) EDS derived elemental composition of ZnO nanostructures deposited at different gas mixing ratios

Element	Atomic %	Atomic % Error	Weight %	Weight % Error
(50:50)				
O	34.7	0.5	8.5	0.2
Zn	59.2	0.3	82.7	0.5
C	6.1	0.2	8.8	0.7
(55:45)				
O	44.9	1.2	13.4	0.5
Zn	45.1	0.7	84.2	1.1
C	10.0	0.5	12.4	0.8
(80:20)				
O	35.6	1.3	13.9	0.5
Zn	56.2	0.9	86.1	1.3
C	8.2	0.6	10.0	0.9

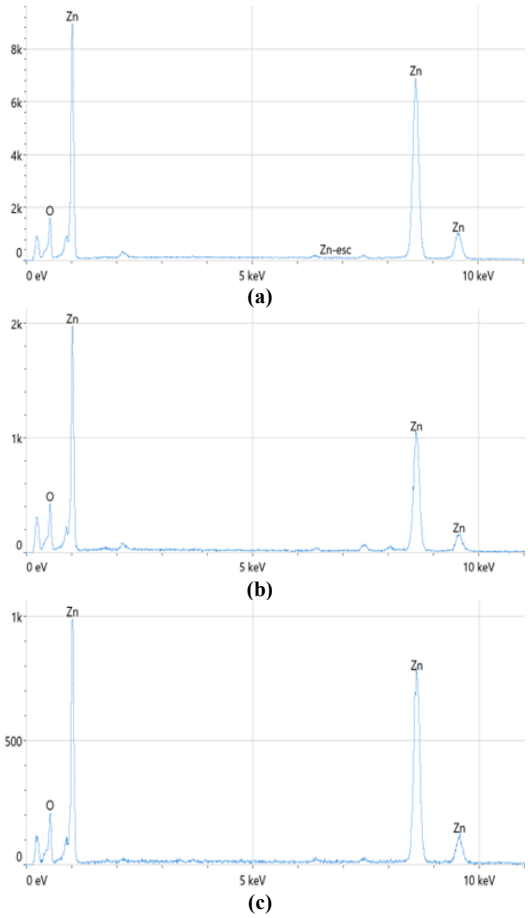

Fig. (5) EDS spectra of the zinc oxide thin films prepared via DC magnetron plasma sputtering at Ar:O_2 mixing ratios (a) (50:50), (b) (55:45), (c) (80:20)

Atomic force microscopy (AFM) was adapted to examine the morphology of the surface and grain size distribution of ZnO nanostructures deposited at the three optimum gas mixing ratios (50:50, 55:45, and 80:20) via reactive magnetron plasma sputtering. The 2D topographic image in Fig. (6a) revealed a moderate smooth surface with mostly grains below 100 nm and limited aggregation with an arithmetic mean height (Sa) of 2.398 nm, while the ratio of 55:45 in Fig. (6b) undergo an increase in the number and size of grains with rougher texture with Sa value of 2.53 nm. On the other hand, the gas ratio of 80:20 in Fig. (6c) reveals a notably change in morphology with shifting toward medium and large grains under Ar-rich environment that having Sa value of 13.9 nm.

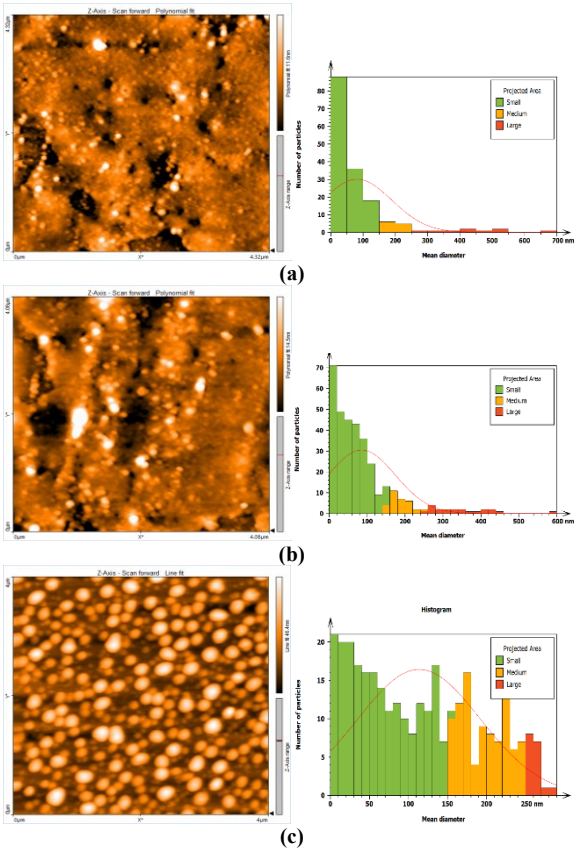

Fig. (6) Topography images of ZnO thin films prepared via DC magnetron sputtering using (a) (50:50), (b) (55:45), and (c) (80:20) gas mixing ratios

So as a comparative analysis the balance gas ratio showed the ZnO films tend to form smoother surface with smaller grains. A slight increase in the Ar content produces denser structures. The rich Ar environment (80:20) promote the roughness resulting in larger grains and higher surface area, this can be attributed to increasing the energy transfer to Zn atoms from Ar ions leading them to highly diffuse through the film. This tunability highlights the important role of gas mixing ratio in customizing ZnO nanostructures for specific applications.

The wavelength dependence of optical absorbance and reflectance spectra of the deposited ZnO films by reactive magnetron plasma sputtering are shown in Fig. (7a). The first observation of UV-Visible spectra indicates all samples exhibit strong absorption in the UV region, and minimum of over 96% in the visible range, this could be assigned to wide band gap in addition to smoother surface morphology of the prepared films. The strong absorption band activated in the UV region are concentrated around 350 to 360 nm, after that a sharp fall in absorbance after the UV region

 © ALL RIGHTS RESERVED

(beyond 400 nm) reporting a transparent material to visible and near IR light. The reflectance spectra show contrary trends, with low reflectance in the UV region and gradual stabilization towards longer wavelengths.

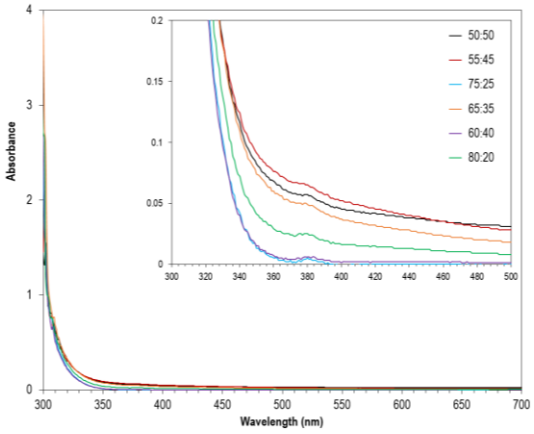

(a)

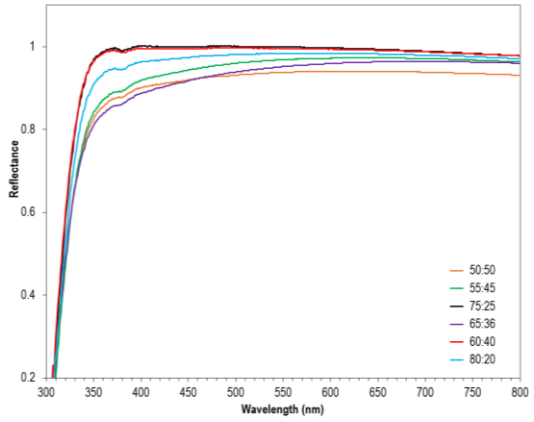

(b)

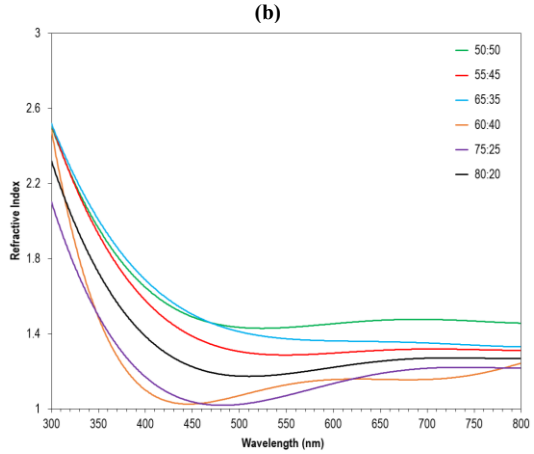

(c)

Fig. (7) Optical properties of the sputtered zinc oxide films prepared using (50:50), (55:45), (60:40), (65:35), (75:25), and (80:20) Ar:O_2 mixing ratio: (a) Absorption spectra, (b) Reflection spectra, and (c) Variation of refractive index with wavelength

The refractive index (n) of the ZnO nanostructures is illustrated in Fig. (7b). For all samples n decreases rapidly in the ultraviolet (UV) range and then stabilize in the visible spectrum. The refractive index range between 1.2 and 2.0, emphases the nanophotonic relevance of deposited ZnO films spurting their applicability in optical coating and waveguide layers. The optical homogeneity of the synthesized ZnO film is clear by noticing the dispersion curve in Fig. (7b) where nearly invariant behavior of the refractive index in the visible spectral region (400-700 nm) with values confined between 1.11 and 1.56.

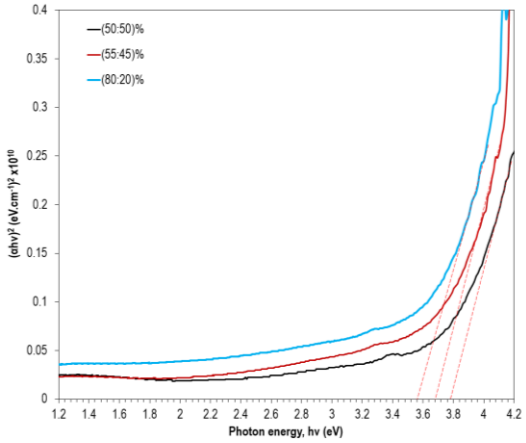

Fig. (8) Determination of optical band gap of the sputtered zinc oxide thin films prepared using (50:50), (55:45), and (80:20) Ar:O_2 mixing ratios

The energy of the optical band gap (Eg) of the deposited ZnO films has been calculated via the Tauc expression [25]. It is found to be in the UV range and has a values of (3.56-3.78) eV, as shown in Figure 8. It was noted that band gap decreases with decreasing oxygen content. This behavior can be ascribed to the presence of vacancies of oxygen resulting in Ar rich environment that enhance Zn sputtering and limit oxygen availability for reaction. They behave as electron traps and introduce localized states within the band gap. These vacancies-induced states enable the valence and conduction bands electronic transitions, thereby narrowing the effective band gap.

Conclusion

ZnO nanostructures were produced via reactive magnetron plasma sputtering with structural, optical, and morphological characteristics strongly influenced by Ar:O_2 gas ratio. XRD results revealed that the ratio (80:20) % produced smallest crystallite size and highest microstrain due to oxygen vacancies induced lattice distortion. AFM showed a marked increase in roughness from 2.398 nm (50:50) % to 13.91 nm (80:20) % accompanied by a shift toward larger grains under Ar rich conditions whereas oxygen rich nanostructures favor finer and smoother surface morphologies. High transparency in addition to wide band gap range from (3.56-3.78 eV) decreasing with reduced oxygen content. These findings highlight the importance of utilization of reactive magnetron sputtering in synthesis high quality and purity ZnO

 © ALL RIGHTS RESERVED

materials that are potential for many important applications.

References

[1] M.A. Borysiewicz, "ZnO as a functional material, a review", *Crystals (Basel)*, 9(10) (2019) 505.

[2] D. Fischer, D. Zagorac and J.C. Schön, "Fundamental insight into the formation of the zinc oxide crystal structure", *Thin Solid Films*, 782 (2023) 140017.

[3] M.A. Faisal, S. Ahmed and M.A.B.H. Susan, "Nanostructured ZnO with Tunable Morphology from Double-Salt Ionic Liquids as Soft Template", *ACS Omega*, 9(11) (2024) 12992-13005.

[4] Y. Sun et al., "The applications of morphology controlled ZnO in catalysis", *Catalysts,* 6 (2016) 188.

[5] A. Mclaren et al., "Shape and size effects of ZnO nanocrystals on photocatalytic activity", *J. Am. Chem. Soc.*, 131(35) (2009) 12540-12541.

[6] J.-W. Hoon et al., "Direct current magnetron sputter-deposited ZnO thin films", *Appl. Surf. Sci.*, 257(7) (2011) 2508-2515.

[7] Q. Li et al., "Photoluminescence and wetting behavior of ZnO nanoparticles/nanorods array synthesized by thermal evaporation", *J. Alloys Compd.*, 560 (2013) 156-160.

[8] M.S. Al-Assiri et al., "Synthesis, structural and electrical properties of annealed ZnO thin films deposited by pulsed laser deposition (PLD)", *Superlatt. Microstruct.*, 75 (2014) 127-135.

[9] N.B. Patil, A.R. Nimbalkar and M.G. Patil, "ZnO thin film prepared by a sol-gel spin coating technique for NO_2 detection", *Mater. Sci. Eng. B*, 227 (2018) 53-60.

[10] S.A.H. Abbas, E.S. Hassan and O.M. Abdulmunem, "Growth of different zinc oxide nanostructures under hydrothermal pH values", *Baghdad Sci. J.*, 21(7) (2024) 6.

[11] A. Hadi and N. Abbas, "Influence of Using Different Preparation Methods on the Properties of ZnO Nanoparticles", *Iraqi J. Phys.*, 23(2) (2025) 54-63.

[12] A.A. Baqer, N.J. Ghdeeb and N.A. Hussain, "Photocatalytic Degradation of Methylene Blue Dye Using Zinc Oxide Nanoparticles Prepared by Green Synthesized", *Baghdad Sci. J.*, 22(5) (2025) 1586-1595.

[13] S. Faisal et al., "Green synthesis of zinc oxide (ZnO) nanoparticles using aqueous fruit extracts of Myristica fragrans: their characterizations and biological and environmental applications", *ACS Omega*, 6(14) (2021) 9709-9722.

[14] T.S. Mahdi and F.J. Kadhim, "Effect depositions parameters on the characteristics of $Ni_{0.5}Co_{0.5}Fe_2O_4$ nanocomposite films prepared by DC reactive magnetron Co-sputtering technique", *Iraqi J. Phys.*, 18(45) (2020) 76-88.

[15] E. Slavcheva et al., "Effect of sputtering parameters on surface morphology and catalytic efficiency of thin platinum films", *Appl. Surf. Sci.*, 255(13-14) (2009) 6479-6486.

[16] O.A. Hammadi, M.K. Khalaf and F.J. Kadhim, "Silicon nitride nanostructures prepared by reactive sputtering using closed-field unbalanced dual magnetrons", *Proc. Instit. Mech. Eng. L: J. Mater.: Design Appl.*, 231(5) (2017) 479-487.

[17] J. Maalmarugan et al., "In situ grown ZnO nanoparticles using Begonia leaves–dielectric, magnetic, filter utility and tribological properties for mechano-electronic applications", *Appl. Phys. A*, 128(3) (2022) 217.

[18] H.A. Thabit et al., "Investigation of the thermoluminescence dosimeter characteristics of multilayer ZnO(300nm)/Ag(50nm)/ZnO(x) thin films for photonic dosimetry applications", *Opt. Mater.*, 137 (2023) 113548.

[19] P. Bharathi et al., "Growth and influence of Gd doping on ZnO nanostructures for enhanced optical, structural properties and gas sensing applications", *Appl. Surf. Sci.*, 499 (2020) 143857.

[20] H. Dong et al., "Ultraviolet lasing behavior in ZnO optical microcavities", *J. Materiomics*, 3(4) (2017) 255-266.

[21] T. Zou et al., "Sensitive and selective n-butanol gas detection based on ZnO nanocrystalline synthesized by a low-temperature solvothermal method", *Physica E: Low Dimen. Syst. Nanostruct.*, 103 (2018) 143-150.

[22] B. Kumar and S.-W. Kim, "Energy harvesting based on semiconducting piezoelectric ZnO nanostructures", *Nano Energy*, 1(3) (2012) 342-355.

[23] A.M. Kasumov et al., "Photocatalysis with the use of ZnO nanostructures as a method for the purification of aquatic environments from dyes", *J. Water Chem. Technol.*, 43(4) (2021) 281-288.

[24] V. Lakshmi Prasanna and R. Vijayaraghavan, "Insight into the mechanism of antibacterial activity of ZnO: surface defects mediated reactive oxygen species even in the dark", *Langmuir*, 31(33) (2015) 9155-9162.

[25] A. Ranjbari et al. "Effect of oxygen vacancy modification of ZnO on photocatalytic degradation of methyl orange: A kinetic study", *Catalysis Today*, 427 (2024) 114413.

 © ALL RIGHTS RESERVED